Effects of Earth Encounters on the Physical Properties of Near-Earth Objects

April 6, 2014

Abstract

ABSTRACT GOES HERE

TODO:

- abstract
- future work section

Part I

Introduction

Earth encounters are known to affect the properties of near-Earth objects (NEOs) through tidal effects. Binzel et al. (2010) showed that weathered surfaces of asteroids are 'refreshed' upon an Earth encounter, causing less reddening to be observed than would otherwise be expected. Richardson et al. (1998) conducted numerical simulations which showed that the tidal forces encountered by Earth-crossing asteroids may cause mass shifting and removal during a flyby, resulting in changes such as distortions, fragment trains, and orbiting ejecta. Rotation in particular was studied by Takahashi et al. (2013) on the asteroid Toutatis, who showed that there was a significant shift in rotational angular momentum during periodic flybys.

Rotational period and asteroid shape are properties which may be extracted from a photometric light curve after a period of observation. Furthermore, the brightness of individual asteroids varies due to changes in heliocentric and geocentric distance, rotation, and solar phase angle (Harris and Lupishko, 1989). The changes due to distance are generally removed during data reduction by using a 'reduced magnitude' value, but the periodic changes in brightness due to rotation and phase angle yield important information regarding the physical properties of the asteroid.

Rotational periods, or spin rates, may tell us about the structure and collision history of an asteroid, while light curve amplitudes may tell us about the shapes of asteroids. Most larger asteroids (0.15 km $<$ D $<$ 10 km) are thought to be 'rubble piles' held together by self-gravity,

since a spin rate barrier appears to exist, as larger asteroids do not appear to spin faster than this "barrier" rate (Pravec et al., 2002). As spin states asymptotically approach rotation around the principal axis of maximum moment of inertia, asteroid light curves are expected to be at least double-peaked, with the exception of near-spherical or other degenerate cases. Light curve amplitudes are indicative of asteroid shapes because elongated asteroids may have greater variation between the least amount of light that it reflects and the most that it reflects.

This thesis expands on the work done on asteroid-Earth encounters by examining the effects of Earth encounters on asteroid rotational periods and amplitudes. To approximate the probability of Earth encounters, the minimum orbit intersection distance (MOID) parameter was used. MOID is defined as the distance between the closest points of two bodies' osculating orbits. Here, MOID is a better parameter to use than the direct geometric distance between the Earth and the objects because the integration of an object's position in its orbit loses precision much faster than information about the orbit itself. This lends greater value to using MOID for timescales on the order of centuries or more. It is important to note, though, that MOID provides an estimate of the lower bound of the distance of an encounter. It does not guarentee that an encounter occurs, but simply suggests an increased likelihood with a lower value. Instantaneous MOID may be determined from the present-day orbital parameters of an object, and was used here as a first-pass look at the relationship between encounters and period/amplitude. A more in-depth look involved conducting a MOID calculation by integrating the orbit of a particular object back into the past to determine how gravitational perturbations may have changed the MOID to its present-day value. This thesis uses photometric and astrometric data from an ongoing asteroid survey (MANOS, decribed **IN SECTION XY.Z**) to extract rotational periods, rotational amplitudes, and MOID for small (D $<$ 1 km) NEOs.

TODO - rewrite this paragraph as things change

Part II presents the background of NEO populations, the effects of planetary encounters on NEO rotational dynamics, and describes the survey from which this thesis draws much of its data. Part III presents an automatic light curve fitting method developed for as part of this project, particularly tailored for the ongoing nature and specific targets of MANOS. Finally, Part IV presents the results obtained from the Earth encounter analysis of this population of asteroids.

Part II

Background

1 The NEO Population

Asteroids, comets, and large meteoroids whose orbit intersects or nearly intersects Earth's are classified as Near-Earth Objects (NEOs). These objects are typically divided into three major categories based on their orbital elements: the Aten, Apollo, and Amor groups, which are collectively known as the AAA asteroids (Shoemaker et al., 1979). Atens are defined as objects having a semimajor axis $a < 1.0$ and an aphelion distance $Q \geq 0.983$ (the perihelion distance of Earth). This classification means that Aten objects only sometimes cross the orbit of Earth. Apollos are defined to have an $a \geq 1.0$ and a perhelion distance $q \leq 1.0167$ (the aphelion distance of Earth). Amors are defined solely by their perhelion distance, namely $1.1067 \leq q \leq 1.3$, meaning they are near-Earth-crossers but do not currently qualify as Earth-crossing asteroids. An NEO is considered a potentially hazardous object (PHO) if its minimum orbit intersection distance (MOID) is less than 0.05 AU and has an absolute magnitude of 22.0 or less (JPL, 2014). Orbital perturbations may, naturally, change the classification of any particular NEO between these groups.

The orbital characteristics of NEOs generally mean that they stay as NEOs for at most a few million years, eventually crashing into the Sun or terrestrial planets, or being flung out of the solar system. The fact that the number of NEOs has remained steady over the last 3 billion years suggests that there is a source of resupply for the population (Bottke Jr et al., 2002). It is believed that main belt asteroids (MBAs) provide the bulk of NEO resupply, with Jupiter and Saturn resonances causing asteroids to move from main belt to NEO orbits. Smaller NEOs are likely collision fragments from MBAs, and exhibit younger (less-weathered) surfaces due to the difficulty of surviving further collisions or planetary ecounters (Binzel et al., 2002).

The NEO population is of special interest planetary astronomers because of its proximity to Earth. NEOs with low inclination and low eccentricity in particular are some of the best solar system targets for space missions due to the relatively low ΔV and short time frame required to reach them. Additionally, the inner solar system orbits and periodic proximity to Earth of these NEOs mean that thermal and power considerations for rendezvous and flyby missions can be significantly simplified compared to near-Sun or outer solar system missions, making them relatively low-cost and within the reach of early private-sector space missions (Perozzi et al., 2001).

TODO - define delta-V?

TODO - something about the importance of asteroid investigations

2 Planetary Encounters

Tidal forces encountered near the terrestrial planets cause a number of changes to asteroids. Distortion and disruption have been found to occur with Earth-crossing asteroids in numerical simulations, with results ranging from elongation and mass stripping, to the formation of fragment trains and binary systems. Low-inclination, low V_∞, and long-rotational-period asteroids experienced the most severe effects in these simulations (Richardson et al., 1998, Bottke Jr et al., 1998). Chapman (1978) argues that large, monolithic MBAs may have been fragmented by collisions to form rubble piles. The lack of observed fast-rotating asteroids with absolute magnitudes $H < 22$ suggests that larger NEOs are indeed such rubble piles and have minimal tesile strength, where any additional spin-up would cause disruption. Smaller NEOs, however, may remain monoliths due to the fact that they were spun off from these rubble piles. Fragment trains are generally formed from distortion processes that cause elongation, resulting in a pattern similar to what happened to Comet D/Shoemaker-Levy 9 during its 1992 Jupiter encounter (Shoemaker et al., 1979). Binary systems, on the other hand, are often formed from spin-up, which causes rubble pile asteroids to fling mass off their equators, resulting in an orbiting body. The fact that about half of the observed fast-rotating ($P < 2.2\,h$) NEOs are binary systems supports the idea that Earth encounters cause strong enough disruptions to form binary systems (Pravec and Harris, 2000, Pravec et al., 2002, Walsh and Richardson, 2006).

Planetary encounters have also been shown to cause 'freshening' of the surface of asteroids. This process runs counter to the usual 'space weathering' process whereby asteroids become increasingly reddened. Binzel et al. (2010) showed that Mars- and Earth-crossing asteroids that have closer encounters with the terrestrial planets tend to appear less weathered. This investigation involved using the Minimum Orbit Intersection Distance (MOID) parameter as a measure of the possibility of an Earth encounter, showing that for an integrated MOID, objects that likely had planetary encounters over the past 500,000 years showed less signs of weathering than objects that were kept away from a planetary encounter (perhaps by orbital resonance) (Binzel et al., 2010).

Numerical simulations across a distribution of asteroid spin states showed that while planetary encounters may cause either spin-up or spin-down or tumbling in individual asteroids, there is an overall trend towards spin-ups, one that is particularly prevalent for bodies with a slow initial rotation (Scheeres et al., 2004). Tumbling cases may be created only if the flyby occurs out of the asteroid's equitorial plane, as gravitational forces along the plane would at most cause a spin-up or

spin-down (Scheeres et al., 2000).

Recently, radar imaging of 4179 Toutatis- an asteroid that makes periodic near-Earth flybys- gave a series of observations that showed terrestrial tidal torques altering the rotational dynamics of the asteroid. These torques mostly caused changes in orientation as the asteroid passed close to the Earth, but a particularly close encounter in 2004 demonstrated a significant perturbation in the angular momentum of the asteroid that persists to the present (Takahashi et al., 2013).

3 Asteroid Surveys

New technologies have shifted to observing focus from larger, multi-kilometer-sized MBAs and NEOs to smaller sub-kilometer-sized NEOs. Asteroid surveys in the past have been able to find and characterize thousands of main-belt and near-Earth asteroids. Many past surveys focused on discovery, with examples including LONEOS, LINEAR, Catalina, and Pan-STARRS. Some studies were specifically for characterization of known objects, such as the albedo characterization done by IRAS, WISE and Akari, and the spectral characterization done by SMASS. These surveys were able to extensively sample the population of asteroids that is larger than the rubble pile limit; however technological limitations meant that they were biased towards being able to observe larger, brigher objects, rarely being able to resolve asteroids dimmer than 22nd absolute magnitude (Binzel et al., 1989, Jedicke et al., 2002).

The past decade has seen a rapid increase in the number of detected NEOs, partly due to advances in observation and computing technologies, but also because of a mandate by the American government to characterize 90% of NEOs larger than 1 km that may present an impact hazard (Binzel et al., 2002). A new, multi-year program started in August of 2013 called the Mission Accessible Near-Earth Object Survey (MANOS) seeks to leverage advances in observing capabilities to characterize asteroid targets that are more than an order of magnitude smaller than those covered by previous studies. It is specifically focusing on sub-kilometer-sized targets that would be accessible by space missions utilizing conventional chemical propulsion, providing rough characterization of targeted NEOs via astrometry, light curves, and spectra. Mission-accessible is defined to be having a $\Delta V < 7$ km/s, which is the approximate limit of conventional chemical propulsion. The program aims to characterize approximately 100 NEOs per year, meaning that there will be a large throughput of data during the survey period, which is expected to last 3 to 5 years. This thesis draws much of its data from the MANOS dataset, and a part of the work done for the thesis was development of automated data processing software for the MANOS pipeline.

Part III

Light Curve Fitting

In order to automate part of the data processing done on incoming MANOS data, a fitting routine, manosCurveFit, was developed by the author to automatically scan reduced MANOS photometry data and convert them into a light curve model which provides the period and amplitude. Before this work, curve fitting for MANOS was done using software built on MATLAB, which contained some components that were relatively poorly documented and required a proprietary platform. Other common fitting methods, such as Canopus, were similarly based on proprietary software. manosCurveFit was developed from scratch specifically for the MANOS data pipeleine and represents one of very few pieces of light curve fitting software that is free and open source, and possibly the only such software that is tailored for asteroid fits.

1 Software Details

1.1 System Overview

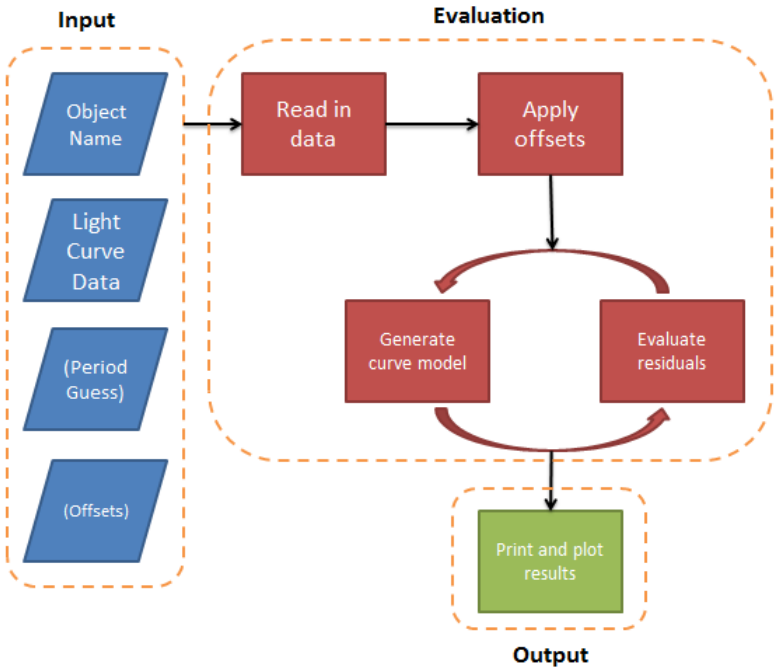

Figure 1: Flowchart showing the conversion from raw data to fitted plots. The dashed boxes represent the three main parts of the software.

The fitting routine fits a mathematical model to light curve data. The fitting process may be generally divided into input, evaluation, and output portions. The inputs in parentheses are not required for the fitting to work, but a guess at the rotational period may significantly constrain the search space, and if data is taken over multiple nights and/or by different instruments, offsets are required to normalize the magnitudes to some baseline. A number of other inputs may also be supplied to constrain or expand the search space. These inputs may be supplied by the fitInfo file for each object. The light curve data is then read in from one or more text files with standardized columns.

Two kinds of magnitude offsets are then applied: offsets by night/instrument, if provided, and a normalizing offset which subtracts the weighted average magnitude of the set from the entire set. The normalizing offset is necessary in order to center the data points on the y-axis for fitting purposes, and may be used in this context because only differential magnitudes are needed. This acts as a coarse adjustment for y-axis centering. A finer adjustment is made by a y-axis offset for the model, which is taken to be part of the least squares minimization. For each period to be checked, a least squares minimization is performed for each order of Fourier coefficients from two to six, unless specified otherwise in the fitInfo file. The parameters that generate the best fit to the data are kept and printed at the end, along with the light curve and residual plots.

See the Appendix for further software documentation.

2 Fitting Rationale

This fitting routine is based on equations 1, 2, and 3 from Harris and Lupishko (1989) (equations 1, 3, and 4, below). The model is based on the Fourier Series

$$H(\alpha,t) = \bar{H}(\alpha) + \sum_{L=1}^{m} A_L sin\frac{2\pi L}{P}(t-t_0) + B_L cos\frac{2\pi L}{P}(t-t_0), \tag{1}$$

where $\bar{H} = 0$ because absolute magnitudes are not necessary for MANOS, and m (the series order), P (the period), and A_L and B_L (the Fourier coefficients) are free parameters. Since a fine-adjustment y-shift is also added, the actual fitting equation becomes

$$H(\alpha,t) = y + \sum_{L=1}^{m} A_L sin\frac{2\pi L}{P}(t-t_0) + B_L cos\frac{2\pi L}{P}(t-t_0), \tag{2}$$

where y is an additional free parameter, which generally takes on a small value.

The residual of a particular observation i may be obtained by

$$\frac{\delta_i}{\epsilon_i} = \frac{V_i(\alpha_j) - H(\alpha_j, t_i)}{\epsilon_i}, \tag{3}$$

where α_j is the reference phase angle on the j^{th} night, t_i is the time of the i^{th} observation, and ϵ_i is the error of the measurement. In the context of NEOs, the phase angle may very well change, particularly as targets pass very close to Earth. However, the majority of MANOS targets will be observed for a short enough period of time (on the order of a few hours) that α will be assumed to be a constant. As such, manosCurveFit does not take phase angles into account. The least squares minimization is then performed on the bias-corrected variance, given by

$$s^2 = \frac{1}{n-k} \sum_{i=1}^{n} \left(\frac{\delta_i}{\epsilon_i} \right)^2 = minimum, \tag{4}$$

where n is the total number of observations, $k = 2m + 1$, where m is defined in 1. The total number of nights of data is also added into k in the form that Harris et al. use, but here, this again needs not be considered because we are concerned with differential photometry, and offsets for different nights will be provided as necessary.

By default, the program will run the fit from $m = 2$ to $m = 6$. The minimum of order two is due to the fact that asteroid light curves are expected to be double-peaked (except for some cases of complex rotation or degenerate cases of near-spherical bodies), and the maximum of order six is used to prevent over-fitting. The curve is centered around zero magnitude by a weighted average of the data, but since there is often still a slight magnitude offset due to the nonuniform nature of the sampling, a magnitude offset parameter was added to allow for a better fit. The user does not normally interact with the optimization of this y-shift parameter.

Precautions were taken to prevent overfitted or unsubstantiated models. Any models which produce amplitudes greater than 2 are rejected. This is necessary to prevent the fit from assuming a model in which the data are a small portion of a much longer period with one or more large spikes where data is not present. As an additional precaution, if the fitted period is more than 25% of the range of the phase-folded data points, a warning is given to notify the user of a potentially under-constrained model.

3 Fitting Results and Data Products

By default, the software automatically produces two figures and a text file report of the fit, which are then saved to the same folder as the data. Examples of these for plots may be seen in Figures 2 and 3. The bottom sub-plot of Figure 2 is an optional plot which shows the residuals of the

generated fit. This plot may be used as an additional manual check on the fit by seeing if any structure or bias remains in the residuals, which may indicate that a higher-order fit is required. Additionally, any significant magnitude bias in the residuals plot may indicative of an incorrect offset of a particular night, if multiple nights' data are used (this effect should also be viable in the main fitted plot). Figure 3 shows the RMS values of different periods that were attempted during the fitting process, with the fit that provided the minimum RMS value representing the fit that was eventually accepted. These figures represent a set of data that was composed of 12 nights, split into two input text files, all of which were automatically merged and processed by the program. This kind of dataset is more complex than most typical MANOS datasets, which will generally be data from a few hours on one instrument for a single night, so multiple input files and automatic merging will largely be unnecessary.

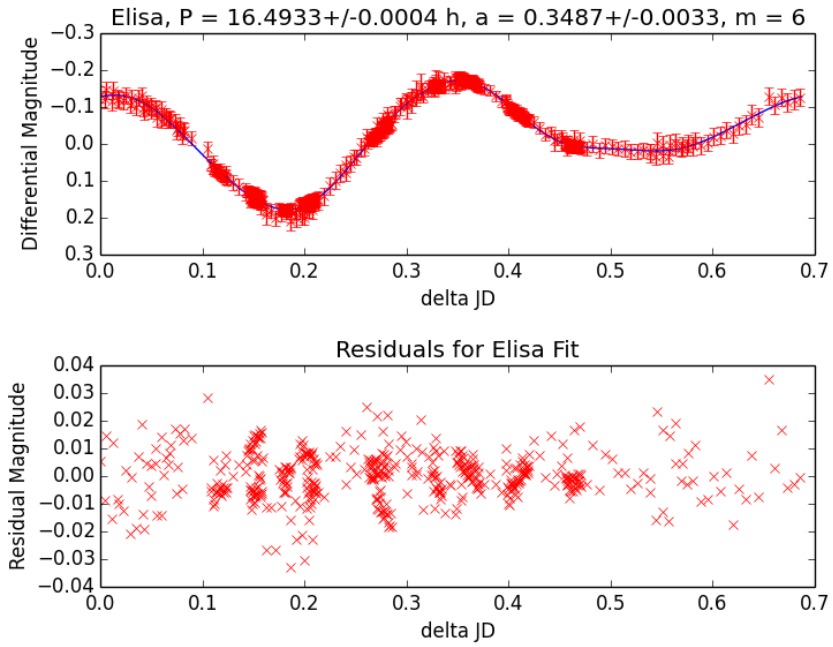

Figure 2: One of the figures produced by manosCurveFit, showing the data points on top of the fitted model (top) along with the residuals of the fit (bottom). The model automatically phase-folded the data to give the best fit, and the residuals here show an example of what would occur for a good fit, since there is no notable bias or structure in the residual plot.

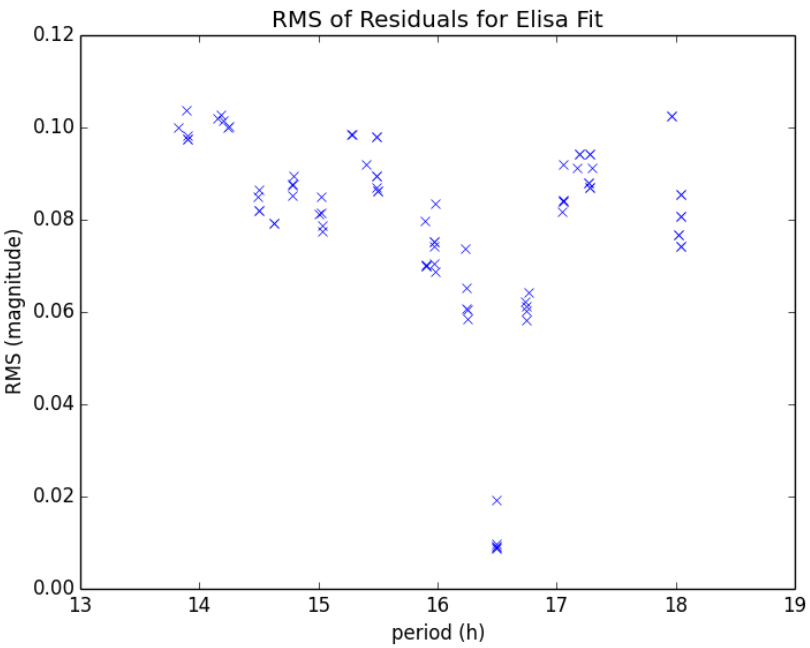

Figure 3: The second figure produced by manosCurveFit, showing the mean RMS values of the fit when different periods are attempted.

The fitting routine was tested against five objects with varying light curve structures, three of which had previously-determined periods. Table 1 shows the comparison between the fitted and accepted periods of the latter three objects, all of which showed very low error values (if any), even though the data used for the fit is only a small subset of the entire set of data used to generate the accepted period. 2579 Spartacus had a different fitted period than accepted period likely due to the fact that the accepted period is based on a much larger baseline of data than what was used for the fit.

Table 1: Period comparisons between fit and accepted values.

Object	Fitted Period (h)	Accepted Period (h)	Error
2012 DA_{14}	5.95 ± 0.12	5.8 ± 0.3	consistent
956 Elisa	16.4933 ± 0.0004	16.494 ± 0.001	consistent
2579 Spartacus	3.812 ± 0.019	3.63599 ± 0.00004	4.84%

Part IV

MOID and Light Curve Comparisons

1 Data Analysis Method

1.1 Minor Planet Center Data Description

Data from the Minor Planet Center's (MPC) light curve and NEO databases were used for a large-population analysis of asteroid properties with respect to MOID values. The MPC's NEO datasets contained information for 827 Aten, 5306 Apollo, and 4500 Amor objects when it was polled for this project in March of 2014, while the light curve database contained 2326 objects. The light curve database had the amplitude and period information for each object, but lacked MOID data, which was contained in the NEO dataset. As such, it was necessary to merge the two sets, cross-referencing objects contained in both to obtain a complete listing of light curve properties and MOID. The resulting set contained 828 objects.

- MPC data for Amor, Apollo and Aten NEOs downloaded (giving orbital parameters)
- MPC light curve database downloaded (giving period)
- the two were separate sets, so targets were matched from one to the other by provisional designation or name

1.2 MANOS Data Description

- explain how MANOS data is obtained

1.3 Data Processing

The resulting dataset was processed to look for differences in the distribution of light curves amplitude and period with respect to MOID. Since MOID presents only a lower bound of the actual intersection distance, a small MOID does not guarantee that an object actually passed near the Earth, but rather only increases the likelihood that it did. As such, objects were grouped by MOID values and then histograms of period and amplitude were produced for each grouping. A difference between the distribution of these histograms from group to group would possibly be an indicator of an effect of a near-Earth encounter on the property being plotted.

The focus of the comparison is between objects with MOID values greater than 0.002 AU and those less than 0.002 AU. This value represent the rough Earth-Moon distance, and gravitational effects from an encounter would likely only be observed in objects closer than a lunar distance.

- cut out objects that are further away- reject all objects with MOID > 0.05 (PHA definition, ~ 19.5 Earth-Moon distances - might need to justify why this limit is good)
- arbitrary MOID value problem - redistribute the MOID artifacts?
- rebin remaining asteroids by MOID
- Amplitude bias correction was performed using the procedure described in Binzel and Sauter (1992). This correction was done to correct for a bias introduced by possible undersampling of the light curves, which would generate a lower estimate of the amplitude. The correction procedure attempts to bring the amplitude estimate as close as possible to what it would be if the object was observed at a 60° phase angle.
- plot histogram of period and amplitude for each MOID bin

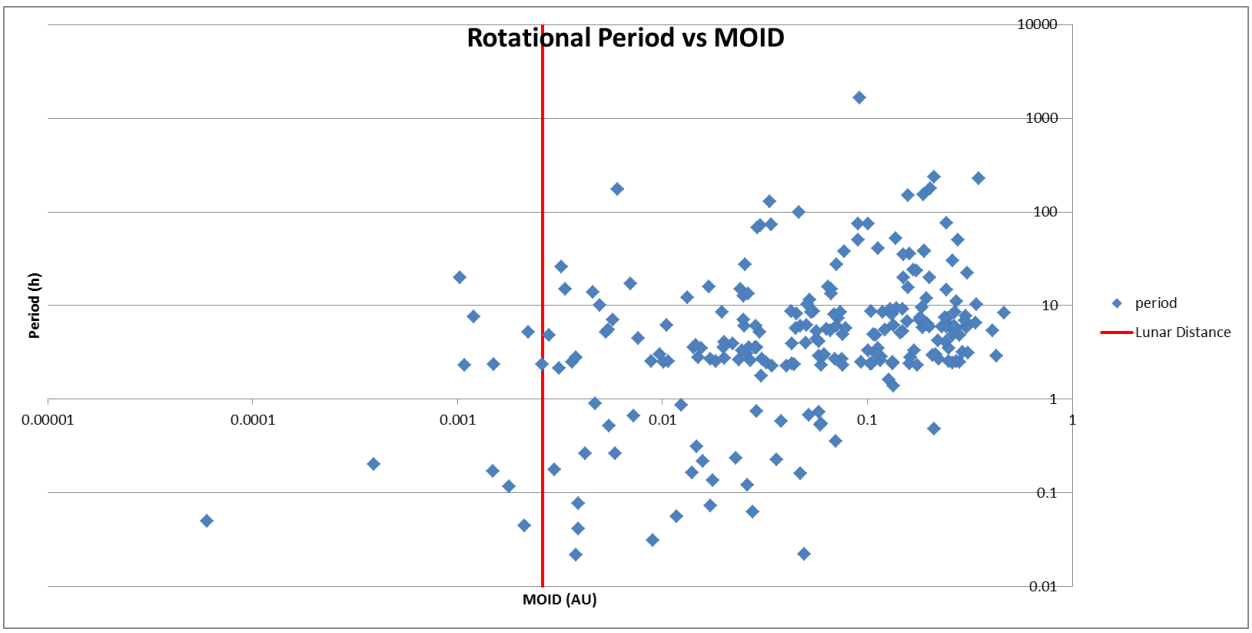

Figure 4: Period vs. minimum orbit intersection distance for Aten, Apollo, and Amor (AAA) NEOs.

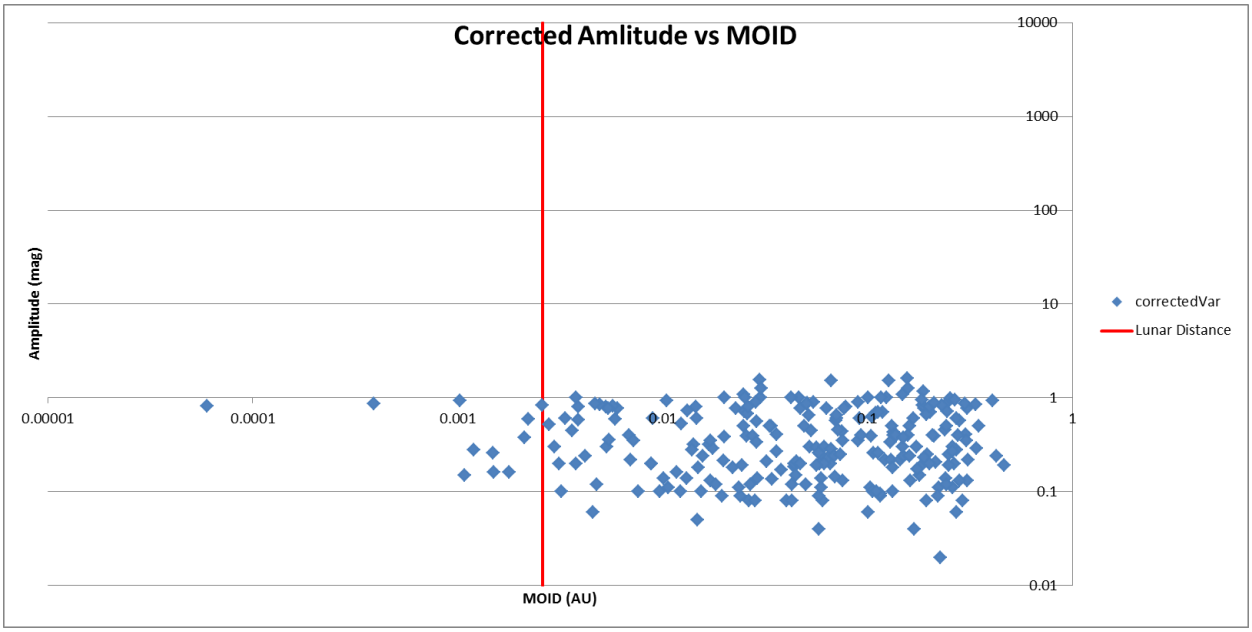

Figure 5: Bias-corrected amplitude vs. minimum orbit intersection distance for Aten, Apollo, and Amor (AAA) NEOs.

FIGURE: scatterplot of previous NEOs with MOID vs instantaneous MOID

FIGURE: change in MOID before and after evolution

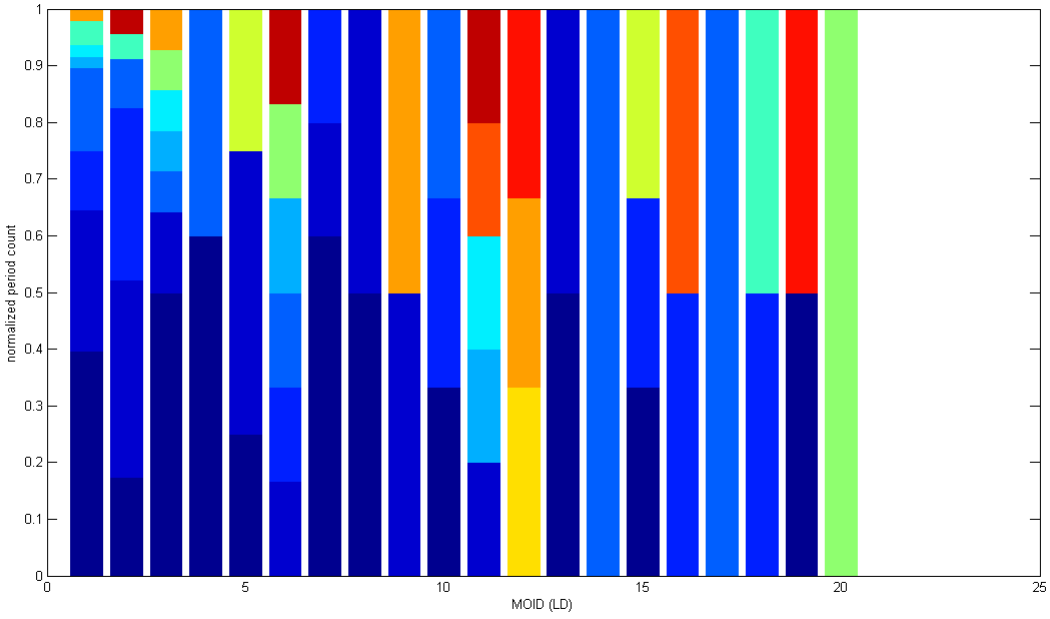

Figure 6: TODO - something like this should probably appear...

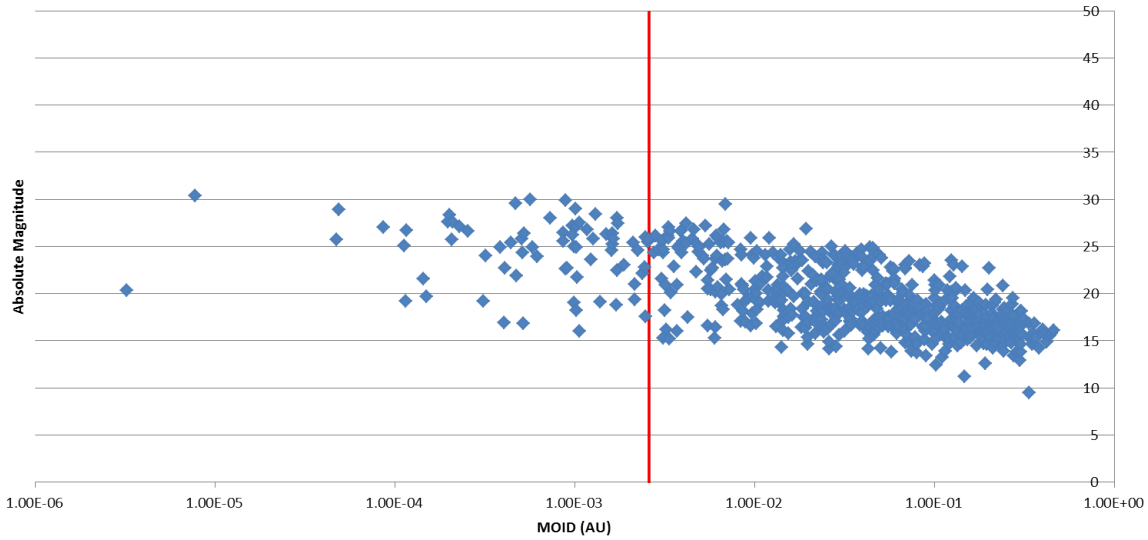

Figure 7:

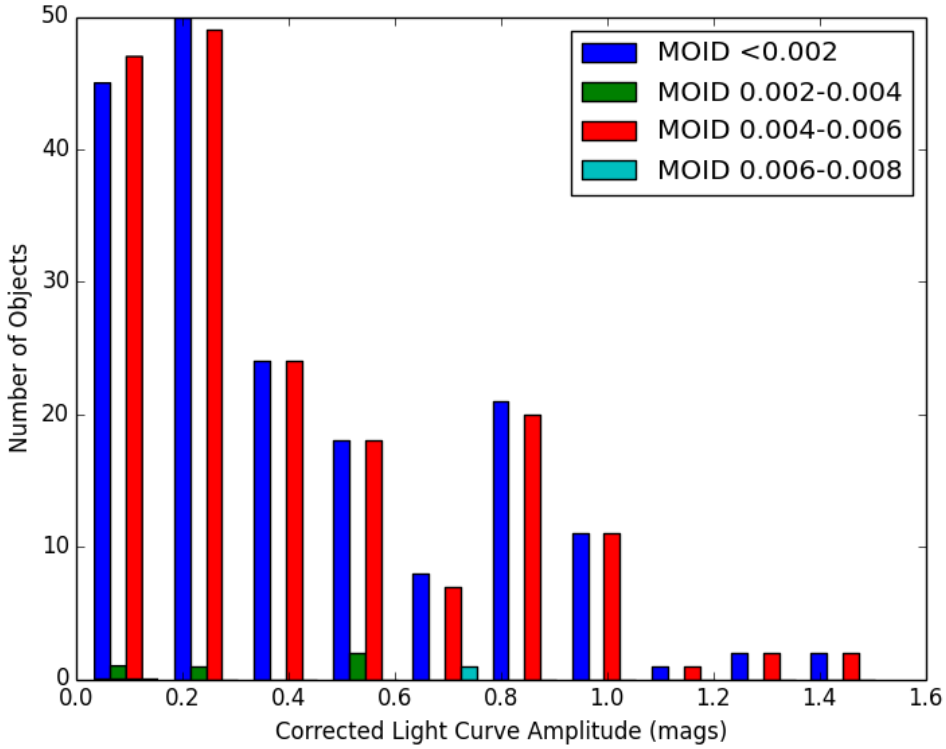

Figure 8: Histogram of objects of different light curve amplitudes, ranging from MOID = 0 to MOID = 0.008.

FIGURE: MOID vs period

Part V

Future Work

References

Richard P Binzel and Linda M Sauter. Trojan, hilda, and cybele asteroids: New lightcurve observations and analysis. *Icarus*, 95(2):222–238, 1992.

Richard P Binzel, Paolo Farinella, Vincenzo Zappala, and Alberto Cellino. Asteroid rotation rates-distributions and statistics. In *Asteroids II*, volume 1, pages 416–441, 1989.

Richard P Binzel, Dmitrij F Lupishko, Mario Di Martino, Richard J Whiteley, and Gerhard J Hahn. Physical properties of near-earth objects. *Asteroids III*, 255, 2002.

Richard P Binzel, Alessandro Morbidelli, Sihane Merouane, Francesca E DeMeo, Mirel Birlan, Pierre Vernazza, Cristina A Thomas, Andrew S Rivkin, Schelte J Bus, and Alan T Tokunaga. Earth encounters as the origin of fresh surfaces on near-earth asteroids. *Nature*, 463(7279): 331–334, 2010.

William F Bottke Jr, Derek C Richardson, and Stanley G Love. Production of tunguska-sized bodies by earth's tidal forces. *Planetary and space science*, 46(2):311–322, 1998.

William F Bottke Jr, Alberto Cellino, Paolo Paolicchi, and Richard P Binzel. An overview of the asteroids: The asteroids iii perspective. *Asteroids III*, 1:3–15, 2002.

CLARK R Chapman. Asteroid collisions, craters, regoliths, and lifetimes. In *NASA Conference Publication*, volume 2053, pages 145–160, 1978.

AW Harris and DF Lupishko. Photometric lightcurve observations and reduction techniques. In *Asteroids II*, volume 1, pages 39–53, 1989.

Robert Jedicke, Jeffrey Larsen, and Timothy Spahr. Observational selection effects in asteroid surveys and estimates of asteroid population sizes. *Asteroids III*, pages 71–87, 2002.

JPL. Neo groups, 2014. URL `http://neo.jpl.nasa.gov/neo/groups.html`.

Ettore Perozzi, Alessandro Rossi, and Giovanni B Valsecchi. Basic targeting strategies for rendezvous and flyby missions to the near-earth asteroids. *Planetary and Space Science*, 49(1):3–22, 2001.

Petr Pravec and Alan W Harris. Fast and slow rotation of asteroids. *Icarus*, 148(1):12–20, 2000.

PETR Pravec, ALAN W Harris, and T Michalowski. Asteroid rotations. *Asteroids III*, 113, 2002.

Derek C Richardson, William F Bottke Jr, and Stanley G Love. Tidal distortion and disruption of earth-crossing asteroids. *Icarus*, 134(1):47–76, 1998.

Daniel J Scheeres, F Marzari, and A Rossi. Evolution of neo rotation rates due to close encounters with earth and venus. *Icarus*, 170(2):312–323, 2004.

DJ Scheeres, SJ Ostro, RA Werner, E Asphaug, and RS Hudson. Effects of gravitational interactions on asteroid spin states. *Icarus*, 147(1):106–118, 2000.

Eugene M Shoemaker, JG Williams, EF Helin, and RF Wolfe. Earth-crossing asteroids: Orbital classes, collision rates with earth, and origin. *Asteroids*, 1:253–282, 1979.

Yu Takahashi, Michael W Busch, and DJ Scheeres. Spin state and moment of inertia characterization of 4179 toutatis. *The Astronomical Journal*, 146(4):95, 2013.

Kevin J Walsh and Derek C Richardson. Binary near-earth asteroid formation: Rubble pile model of tidal disruptions. *Icarus*, 180(1):201–216, 2006.

Appendix

A manosCurveFit System Dependencies

This software was developed and tested on Python 2.7.1, and imports from the following typically pre-installed packages: *operator, os, time, sys*, *string*, and *cmd* and the following typically non-pre-installed packages: *lmfit, matplotlb, numpy* and *uncertainties*.

The latter set of packages are commonly used for scientific applications and stable builds should be easily found.

B manosCurveFit Input, Evaluation, and Output Methods

The software handles data input by reading text files and storing user-defined data columns as numpy arrays in a *lightCurveData* object. Evaluation is handled by the *fitData* function, which utilizes *lmfit*'s minimization routine with free parameters given as Parameter object inputs. Output is handled by the *outputResults* function, which has options to display results in various ways.

B.1 fitInfo Specification

Keyword	Arguments	Meaning
FILES	integer	number of data files for this object (used as a check)
GUESS	string, then 1 or 3 integers	see Guess Specifications section, below
HARDMAXPERIOD	float or int	hard maximum period to not search above
HARDMINPERIOD	float or int	hard minimum period to not search below
OFFSET	string	starts a series of night/offset pairs used by the string specifying the dataset
ENDOFFSETS	N/A	ends the series of offsets (required if OFFSETS are used)

Table 2: fitInfo keywords (all keywords are optional)

Example fitInfo File:

```
FILES 2
# method min max step
GUESS range 14 18 0.25
HARDMAXPERIOD 13
HARDMINPERIOD 20
OFFSET Elisa\elisa_mine_standard.txt
1 0.0
2 -0.04
3 0.464
ENDOFFSETS
OFFSET Elisa\elisa_his_standard.txt
1 -0.324
2 -0.257
3 -0.237
4 -0.194
5 -0.223
6 -0.321
7 -0.246
8 -0.372
9 -0.15
ENDOFFSETS
```

B.2 Guess Specification

Three different ways to specify initial guesses at the period value (in hours) exist.

- range (3 floats or ints) - a range of guesses will be used, following the convention min, max, and step size
  - Example: `GUESS RANGE 0.1 5.5 0.25`
- single (1 float or int) - one initial guess will be used
  - Example: `GUESS SINGLE 2`
- None - if the GUESS line is excluded, an interval from 15 minutes to 5 times the observing window will be used (see section on fitData)

B.3 Command Line Interface

Descriptions of all command line options

- `exit` (no arguments) - exits the program
- `fit` (names of objects to be fit, separated by spaces- must match folder names in the Data directory) - runs a fit on the objects specified, regardless of whether or not they have already been processed
  - Example: `fit Martes Elisa`
- `fitAll` (no arguments, or `'redo'`) - runs fits on all objects in the Data directory that do not have an existing light curve plot; if the `'redo'` argument is provided, all plots are fitted, regardless of any existing fits
- `setFitOptions` (option and value arguments) - sets options used in the fitting routine; multiple options may be set at once
  - `minOrder` (non-negative integer argument) - sets the minimum order to be used in the Fourier fit; default is 2
  - `maxOrder` (non-negative integer argument greater than minOrder) - sets the maximum order to be used in the Fourier fit; default is 6
  - `timer` (boolean) - turns a fitting timer on or off, which measures the amount of time required for each fit, generally for diagnostic purposes
    - Example: `setFitOptions minOrder 3 maxOrder 5 timer true`
- `setOutputOptions` (option and boolean setting arguments) - sets options used in the program output; multiple options may be set at once; all options take booleans
  - `printReport` - whether or not to print the fitting report on the console (default is True)
  - `saveReport` - whether or not to save the fitting report to the object's directory (default is True)
  - `plotFullPeriod` - whether or not to plot the full period as determined by the model; if not, the model will only plot up to the available data (default is True)
  - `plotErrorBars` - whether or not to plot the error bars on the data (default is True)
  - `phaseFoldData` - whether or not to phase fold the data and model (default is True)
  - `plotResiduals` - whether or not to plot the residuals of the data as a subplot of the light curve (default is True)
  - `plotPeriodErrors` - whether or not to plot the mean RMS values the errors as a function of the period attempted (default is True)
  - `showPlots` - whether or not the show the plots (default is False); the plots will always be saved to the object's directory
- `showObjects` (no arguments) - lists the object subdirectories found under Data

C manosCurveFit Class and Function Specifications

C.1 The `lightCurveData` Class

class `lightCurveData`(objectName, fileNamesAndFormat[, offsetsList = None])

Creates a lightCurveData object which is used to read in and manipulate the dataset.
Parameters

- **objectName** (string) - name of the object associated with the dataset
  - Example: 'Spartacus20090130'
  - Stored in lightCurveData.name
- **fileNamesAndFormat** (dictionary of dictionaries) - names of text files to be read in, along with the associated column definitions in the data (format specification)
  - Example:

```
fileName = 'Spartacus20090130_MANOS.txt'
# list of lists specifying ['property',column] in the text file
formatSpec = [['night',0],['jd',3],['diffMag',6],['magErr',7]]
fileNamesAndFormat = {fileName:formatSpec}
```

  - Multiple key/value pairs may be used when multiple text files are to be used
  - `'jd'` (Julian date), `'diffMag'` (differential magnitude), and `'magErr'` (magnitude error) must be specified to run the program, additional properties may also be stored in the `lightCurveData` object
  - Remember that Python indexes from zero, so the left-most column in the text file is column 0
  - Any white space in the text file is considered a delimiter (leading and trailing white space is ignored)
  - Stored in lightCurveData.data
- **offsetsList** (list of dictionaries, `None` = no offsets) - offsets associated with nights in each text file
  - Example: [{1:0.0,2:-0.04,3:0.464}]
  - Key/value pairs must be int/float pairs, where the key is the night number, and the value is the offset
  - Multiple dictionaries may be used when multiple text files are to be used- when this is done, the order of these dictionaries must correspond to the order of the files names and specifications used in `fileNamesAndFormat`
  - Keys may be repeated as long as they are in different dictionaries
  - `'night'` property must be specified in the format to use offsetsList
  - **If more than one night is used for any target, all data must have associated night and offset values**
    - The only case where offsets are not necessary is if the entire dataset came from a single night

C.2 The `fitData()` Function

`fitData`(lightCurveData, fitOptions, method = None[, periodGuess = None[, hardMinPeriod = None[, hardMaxPeriod = None]]])

- **lightCurveData** (lightCurveData object)

- **fitOptions** (dictionary) - the options used in calculating the fit, as specified in `setFitOptions` (see Command Line Interface)
  - `orderMin` - minimum m value to be attempted in the Fourier model, as outlined in the Fitting Rationale section (default is 2)
  - `orderMax` - maximum m value to be attempted in the Fourier model, as outlined in the Fitting Rationale section (default is 6)
  - `timer` - whether or not to measure the amount of time it takes to fit the model (default is False)
- **method** (string) - method to be used for traversing the search space of periods: `None`, `'single'` or `'range'`; supplied by the fitInfo file, when available
  - when method is `None`, a maximum recoverable period is estimated for up to 5 times the observing window; periods are checked at 15 minute (0.25 hour) intervals; periodGuess is ignored in this case
  - when method is `single`, periodGuess must be provided as an int or a float, which serves as the only initial period used in the minimization
  - when method is `range`, periodGuess must be provided as a three-element list of `[start, stop, step]` integers or floats, which is then automatically converted into a list of initial periods for minimization
- **periodGuess** (int or float or three-element list of ints or floats) - the initial period used for minimization, given in hours; this provides a starting point for the the period parameter, which does not remain fixed during the minimization; supplied by the fitInfo file, when available
- **hardMinPeriod** (int or float) - the hard lower limit for the period fitting, no period below this value will be attempted in the evaluation; supplied by the fitInfo file, when available
- **hardMaxPeriod** (int or float) - the hard upper limit for the period fitting, no period above this value will be attempted in the evaluation; supplied by the fitInfo file, when available

Returns (bestFit, bestOrder, periodsTested, periodErrors), where bestFit is a Minimizer object, bestOrder is an int, and periodsTested and periodErrors are corresponding lists of floats.

C.3 The `outputResults()` Function

`outputResults`(fit, m, lightCurveData, outputOptions[, periodErrors = None])

- **fit** (Minimizer object) - the bestFit object returned by `fitData()`
- **m** (int) - the bestOrder returned by `fitData()`
- **lightCurveData** (lightCurveData object) - the lightCurveData object used for this run
- **outputOptions** (dictionary) - the options used in displaying and saving the results of the run, as specified in `setOutputOptions` (see Command Line Interface)
- **periodErrors** (n by 2 list of lists) - when provided, a second figure will be plotted showing the mean RMS of the residuals as a function of period

D manosCurveFit Future Improvements

- add phase angle considerations, pending improvements to the Lowell Observatory orbital parameters database
- polling from the Lowell ephemeris database to specify changes due to orbit
- implement a method to limit the Nyquist maximum recoverable period result, possibly using a periodogram, since it currently may be unreasonably large due to uneven sampling

- generalize the inputs for `lightCurveData.getData()`, which currently can only take in floats, so things such as filters (which may be characters) can't be read in